Landslides Hazard Mapping Using High-Resolution Satellite Data

Saloni Jain, Rakesh Khosa, and A. K. Gosain

Abstract Landslides are one of the severe natural hazards induced by heavy rainfall, deforestation, slope failure and urban expansion. It can lead to significant loss of life and property in hilly and gully regions. Field studies that identify and map landslides are expensive and time-consuming as it includes the cost of the survey, travelling, workforce, and instrument. Although progression in technology and availability of high-resolution remote sensing data has now made it possible to identify landslides (satellite images and aerial photographs), accessibility to high-resolution satellite data is still an expensive and tedious procedure. Several studies have conducted in a GIS environment to map landslide zones, but the resolution of the open-source data is commonly coarse (30 m), which adds to the uncertainty of the outcome. In this study, application of the appropriate rule set with object-based image analysis (OBIA) technique has been used to identify landslides zones, through a combination of spectral, textural and geometrical properties of imagery and topographic data. It overcomes the shortcomings induced by pixel-based classification. For the current study, High spatial resolution data such as Google Earth imagery and CartoDEM (30 m) has been used. This approach shows an excellent prospect for quick and near-to-actual assessment of landslides zones which are generally induced by extreme rainfall events in the hilly regions of India. The methodology used has the potential to facilitate more reliable disaster management strategies. This study shows the potential of open-source data and emerging technology in the field of landslide assessment.

Keywords Landslides · Object-based image analysis · Google Earth

1 Introduction

Landslides count among the most exacting of natural hazards because of its potential to cause loss to human life as well as socio-economic disruption. Landslides occur over the area with sharp changes in relief and generally triggered by a range

S. Jain (✉) · R. Khosa · A. K. Gosain
Department of Civil Engineering, Indian Institute of Technology (IIT), Delhi, New Delhi, India
e-mail: cez178078@iitd.ac.in

M. Latha Gali and P. Raghuveer Rao (eds.), *Geohazards*, Lecture Notes in Civil Engineering 86, https://doi.org/10.1007/978-981-15-6233-4_7

of processes such as rainfall, earthquakes. Due to burst in the human population, anthropological activities are bound to continue to expand into landslide-prone environments; hence, the recognition of the scope and the magnitude of the hazard has increased (Cruden and Varnes 1996; De Blasio 2011; Woebbecke et al. 1995).

It is necessary to predict and map the possible landslide regions in order to mitigate the disaster. Researchers over the decades have presented different ideas about landslide mapping such as landslide inventory mapping is a representation of the spatial distribution of the landslides at a predefined cartographical scale (Malamud et al. 2004; Mayr et al. 2016); landside mapping can be categorised by displacement of vegetation together with unconsolidated material in surveying methods in mountain region (Motohka et al. 2010; Selby 1993).

Geospatial technologies are proven to be "New tool to an Old Problem" in the context of landslides. It can play an essential role in this field such as mapping of past or active slope failures, identifying the possible sites for a landslide, landslide zonation and predicting its time of occurrence. Geospatial technologies provide abilities to study the interrelations and interactions between the various disciplines to reveal the underlying fundamental processes fixed in the images from a distance (Platt and Rapoza 2008). The underline assumption in mapping landslide is the occurrence of this event leaves visible marks on the territory. Recently, detached landslide is easy to recognise on the satellite imagery due to their colour difference from the surroundings as they appear lighter in tone (Tsai et al. 2010; Santurri et al. 2010). However, as clock shifts, it gets harder to identify the boundary of slides due to fuzziness brought by environmental and physical processes, so optical remote sensing promises mapping of only shallow and recent landslides. Due to progressive enhancement in the resolution of satellite imagery, researches have inclined their attention towards the mapping of the landslide by using remote sensing the techniques over the conventional methods. However, the field observations are still the main bases of soil mapping as it captures the three-dimensional properties of Pedon (the smallest unit of soil). Currently, no satellite data ensures this level of detailed information. Advantages and limitations of conventional methods are exhaustively presented in previous reviews (Guzzetti et al. 2012; Weidner 2008).

The development in satellite optical imagery opened up new possibilities in the practice of visual interpretation for landslide investigation. Remote sensing can play an essential role in landslides inventory studies (Weidner 2008), especially in inaccessible and remote regions. The new remote sensing data could provide equivalent results even in areas where landslides have left faded marks only (Fiorucci et al. 2011). Due to the high price of data acquisition, these high-resolution images are generally utilised in a specific small region and are rarely applied in large ones (Guo et al. 2016).

Google Earth (GE) offers a welcome solution to the above-discussed issues; it provides open, high spatial resolution images suitable for landslide mapping. However, Google Earth images are restricted to a three-band colour code (R, G and B), which is expected to inferior the classification performance due to its poor spectral resolution (Zhan et al. 2005). The potential for the classification of spatial characteristics by Google Maps has been underestimated (Drăgut and Eisank 2010). By analysing the tone, texture and geometric features in a GE image, experts can recognise eroded surfaces with high assurance.

Image processing and analysis for marking landslides is a necessary process and wildly used in the field of disaster studies in order to mark the extent of the disaster. Over some time, several methods of feature extraction have been proposed. It includes manual and automatic extraction, later can be further classified as pixel-based and object-based image analysis. Pixel-based image classification classifies based on the brightness value of pixel while the object-based image analysis (OBIA) partition land-cover parcel into image objects and classified by expert rules. Image segmentation algorithms such as the multiresolution segmentation can be applied to create image objects, which serve as the basis for the classification process. A probable solution to the difficulties associated with pixel-based classification could be the need to function at the spatial scale of the things of concern themselves, moderately than depending on the extent of image pixels (Rau et al. 2011); hence, the methods of object-based image analysis (OBIA) for generating and updating geographical information are becoming more critical. Despite the advantages of OBIA, the visual interpretation of ortho-photos or pixel-based classification approaches are still the predominant methods used for mapping landslides. Due to the particular properties of landslides (e.g. shape) and the enhanced resolution of available imagery, pixel-based classification techniques tend to result in noteworthy commission and omission errors (Casagli et al. 2016). The outcomes of OBIA are more sensitive compared to the pixel-based classification process, which generally produces the pepper–salt effect (Sharma 2017; Scaioni et al. 2014). Apart from the mentioned problems, total reliability on brightness value may reduce the accuracy as two pixels with same spatial reflectance might be entirely different types of objects/ features (e.g. building and roads) or two pixels with very different reflectance may be part of the same object type (e.g. different rooftop materials of buildings).

Arithmetic operations with image bands can highlight specific object classes. Vegetation indices are often used to categorise vegetation and separate it from other categories (e.g. bare earth) in satellite data. The Excess Green Vegetation Index (ExG) is one of the most comprehensive indices if only bands in the visible range are presented (Zhan et al. 2005). It uses "panchromatic" brightness layer than brightness value (R, G and B). It was calculated for the multispectral images by dividing the sum of the three spectral bands by the number of bands. For the classification of landslides, this panchromatic layer was valuable exposure of bare ground because landslides appear brighter as compared to their immediate surroundings on the imagery (Hölbling et al. 2015; Mulders 1987).

In this paper, a methodology has been proposed to map shallow, eroded areas with a high level of detail and accuracy using Google Earth imageries and CartoDEM. An object-based image analysis approach is used to classify eroded surfaces from the surroundings, and also a new technique of accuracy assessment is applied which judges the location as well as shapes and size of the extracted objects with reference objects.

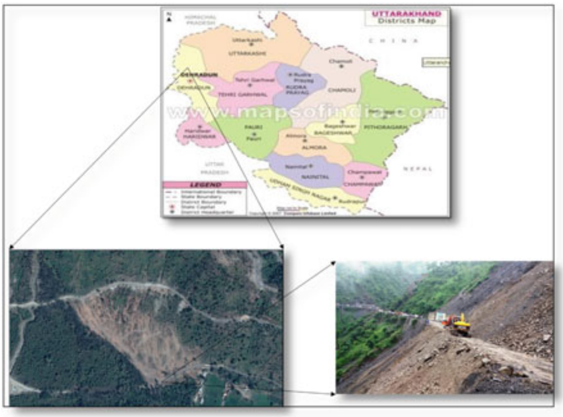

Fig. 1 Study area

2 Study Area and Data

The Kalsi is a beautiful village at the intersection of Yamuna and Tons rivers (Fig. 1). The 79.28 hectare study area is located approximately 49 kms (NE) from Dehradun city, India. It comprises pastoral hill country on moderately indurated Tertiary sandstone and mudstone, with relief in the order of 780 m above sea level. Most of the area falls in the zone of heavy rainfall—as a consequence, rain-triggered shallow landslide erosion is frequent incidence.

Hindustan Times published a report on 13 July 2017, 20:20 IST (Fig. 1) which focuses on the landslides incidences in this Kalsi region of Uttarakhand, especially following heavy monsoon rains and discussed in brief about Kalsi often hold up traffic for several days in the hilly areas. An image of the recent landslide is taken from the Google Earth of the area where the landslides have blocked the path. This portion affected by landslides of Kalsi district has been chosen as a study area. High spatial resolution Google Earth imagery is used, which consists of the spatial resolution 0.5 m. For extraction of drainage pattern and topographical attributes such as slope and elevation, CartoDEM has been used. CartoDEM is a freely available data provided by National Remote Sensing Centre, Hyderabad. The spatial resolution of data is 30 m.

3 Methods

The proposed OBIA methodology for landslide mapping is shown in Fig. 2. The detail of the developed algorithms and how to perform accuracy assessment is described in the following sections.

Fig. 2 Methodology framework for landslide mapping

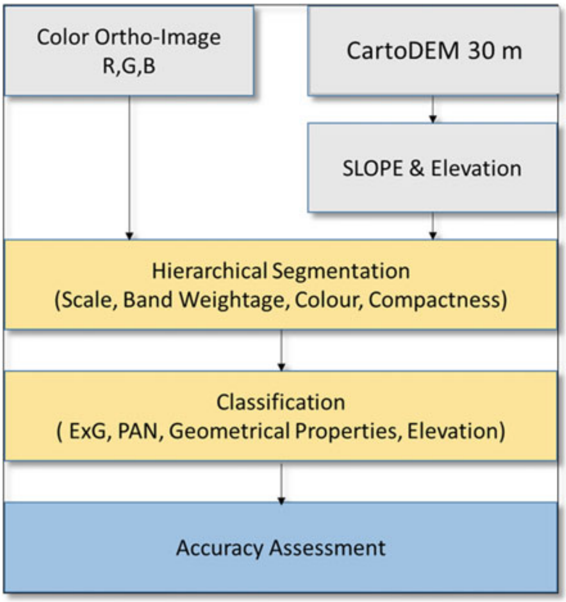

3.1 Segmentation

Image segmentation which is an integral part of OBIA is a process of extraction of the similar objects that subdivide the image into dissected regions (Campbell 2011). The multiresolution segmentation is an optimisation technique which locally minimises the average heterogeneity of image objects for a particular resolution and maximises their respective homogeneity. The segmentation process used in the study is based on region merging algorithm, which begins with one pixel and consecutively merging neighbour pixels, based on the threshold of chosen scale, spectral and shape parameters. A larger-scale parameter will result in more significant-sized image objects. On the other hand, selecting a smaller scale will cause over-segmentation and small objects (Laliberte et al. 2012). Although there are tools available for scale parameter estimation, it is difficult to find a suitable value of the scale parameter without performing the trial-and-error test (Dragut and Blascke 2006).

Other parameters such as colour homogeneity are based on the standard deviation of the spectral values. The shape homogeneity depends on the variation of a compact (or smooth) shape. Homogeneity criteria can be customised by weighting shape and compactness criteria. The shape and colour criterion can be given up to the value of 0.9. This ratio determines the degree shape which influences the segmentation compared to colour—for example, a shape weighting of 0.6 results in a colour weighting of 0.4. In the same way, the value the compactness gives it a relative weighting against smoothness.

Different weights can be assigned to the R, G and B bands by their importance in the mapping. In this study, equal weights have been assigned to all the bands. By trial-and-error method, different sets of values for scale, colour and compactness are run on the images. By observing the outcomes, final sets of parameters for the segmentation have been chosen as scale = 36, shape = 0.8 and compactness = 0.3. The image has a very high spatial (resolution 0.5 m) while a low spectral resolution (3 bands) so more weight is assigned to the shape than colour.

3.2 Visual Interpretation of Landslides

Visual landslide interpretation from the Google Earth was carried out. Each landslide was then subdivided visually into "old landslides" and "new landslides", and also, an effort has been made to separate sediment sources (scars) from areas receiving sediment (debris tails). The ultimate aim of the mapping was to identify all landslides, including old and new landslides.

Regarding spatial location, the feature is well distributed and are covering areas where it could be landslides or in the regions that are landslides, but they have not been mapped due to errors or misinterpretation.

3.3 Classification

Automated thresholding for the classification with spectral features is implemented to the characteristics of each scene individually to classify the imageries.

Excess Green Vegetation Index (ExG)

Excess Green Vegetation Index (ExG; (Mayr et al. 2016; Yu and Gong 2011)) is used to classify eroded surface from the surroundings. Google Earth image consists of the red (R), green (G) and blue (B) colour bands which are used in the estimation of ExG. The mathematical expression of ExG is as follows in Eq. 1.

$$\mathrm{ExG} = 2g - b - r \tag{1}$$

where

$$b = \frac{B}{(B+G+R)} \quad g = \frac{G}{(B+G+R)} \quad r = \frac{R}{(B+G+R)}$$

The data was acquired on 22 October 2017, so according to the phenological cycle of the grass and trees, their colours appear as dark green, while landslide areas appear as shades of brown. By observing the equation, it can understand that more weight is assigned to a green colour, so the object reflects more green band will have higher ExG value and vice versa. As the eroded surface has low reflectivity in the green band, the extracted ExG value is less than zero. These indices work better when there is an enhanced separability between the grass and eroded surface.

Green Red Vegetation Indices (GRVI)

This index is beneficial to extract vegetation from Google Earth images. As these images do not contain NIR band (vegetation tends to have a high reflectance in NIR bands), these indices use only red and green bands for extraction of vegetation (Rau et al. 2011). The mathematical expression for GRVI is as follows in Eq. 2.

$$\mathrm{GRVI} = \frac{\mathrm{Green} - \mathrm{Red}}{\mathrm{Green} + \mathrm{Red}} \tag{2}$$

Its value ranges from -1 to $+1$, which is useful for differentiating forest area from the sparse vegetation as forest area has a higher GRVI value than sparse vegetation. As in the image, sparse vegetation appears brownish; it is very tedious to differentiate sparse vegetation from the eroded surface. Nevertheless, GRVI has a different value for each class as green vegetation (GRVI > 0), soils (GRVI < 0) and water/snow (GRVI close to 0) (Motohka et al. 2010). They are used to remove the sparse vegetation regions from the eroded surface regions.

Panchromatic (PAN)

An arithmetic average was calculated for the multispectral images by dividing the sum of the three spectral bands by three, which is termed as "Panchromatic". For the classification of landslides, this panchromatic layer was significant since landslide regions appear lighter in tone than their immediate surroundings on the photographs due to the removal of existing features which causes the exposure of bare ground (Hölbling et al. 2012). PAN was used to identify the landslides which were left due to positing ExG value. By referring to imagery, recent landslides appear as a bright object which shows that they have higher PAN value.

Other Characteristics

Object-based image analysis has various advantageous over pixel-based classification; it allows the user to work with other properties such as geometric and texture than spectral properties of images. Digital elevation model is used as an ancillary data for landslide detection as landslide generally occurs at steep slopes, so the integration of digital elevation models (DEM) and its derivatives (e.g. slope, drainage pattern) add to the accuracy of the extraction.

Geometrical properties such as length/width ratio are proven to be very useful in the extraction of road feature. In the image, in some places it is difficult to distinguish between the road and eroded surface as they both have high reflectance properties which lead to the misclassification of the way into the eroded surfaces, but road is a linear feature, so its L/B ratio is higher than the other classes. By training the segmentation algorithm according to the mentioned properties, roads can be classified differently from the eroded surfaces.

3.4 Accuracy Assessment

The assessment was carried out by a few parameters of the discrepancy methods. The assessment has done by the reference training object which was digitised manually by visual interpretation of imagery. This method focused on the area parameters of both segmented and reference objects. The area-based method assesses the accuracy of objects based on both location and geometry. Several parameters have been used in the study: (1) the relative area of an overlapped region to a reference object ($\mathrm{RA_{or}}$), (2) the relative area of an overlapped region to a segmented object ($\mathrm{RA_{os}}$), (3) the quality rate (qr), (4) the SimSize, given as below (Taylor et al. 2015). Each factor judges the efficiency of segmented objected concerning the reference object. The mathematical expression of each element is shown in Eqs. 3, 4, 5 and 6, respectively.

$$\mathrm{RA_{or}}\% = \frac{1}{n}\sum_{i=1}^{n}\frac{A_{\mathrm{o}}(i)}{A_{\mathrm{r}}} \times 100\% \tag{3}$$

$$\mathrm{RA_{os}}\% = \frac{1}{n}\sum_{i=1}^{n}\frac{A_{\mathrm{o}}(i)}{A_{\mathrm{s}}(i)} \times 100\% \tag{4}$$

$$\mathrm{qr} = \frac{1}{n}\sum_{i=1}^{n} 1 - \frac{A_{\mathrm{o}}(i)}{A_{\mathrm{u}}(i)} \tag{5}$$

$$\mathrm{SimSize} = \frac{1}{n}\sum_{i=1}^{n}\frac{\min\left(A_{\mathrm{r}}, Aa_{\ S(i)}\right)}{\max\left(A_{\mathrm{r}}, A_{S(i)}\right)} \tag{6}$$

where n is the number of segmented objects created by an algorithm. A_{r} is the area of the reference object, A_s is the area of the ith segmented object, $A_{\mathrm{o}}(i)$ is the area of the ith overlapped region associated with the reference object, and $A_{\mathrm{u}}(i)$ is the area of the union between the references object and the ith segmented object. $\mathrm{RA_{or}}$ and $\mathrm{RA_{or}}$ assess the accuracy by measuring the overlay region between the reference and segmented objects. When objects are well-segmented, the overlapping area will be more so both $\mathrm{RA_{or}}$ and $\mathrm{RA_{os}}$ values will be close to 100. The quality rate parameters focus on both the geometry and location of the segmented objects. qr parameter (Weidner 2008) ranges between 0 and 1. The values close to zero indicate a perfect match while values close to one indicate an over- or under-segmentation. The SimSize (Zhan et al. 2005) measures the similarity regarding the size of the segmented object. It ranges between 0 and 1, with one being ideal. It assesses how accurately segmented objects have preserved the shape of the feature. The more same object will have a higher value (close to 1) and vice versa.

4 Results and Discussions

The outcome of the study is divided into two portions, as follows: landslide mapping and accuracy assessment.

4.1 Landslides Mapping and Factors Affecting

A necessary input to perform classification is objects. Objects are the group of the pixel that shares similar characteristics according to a prespecified threshold. Segmentation is performed to convert pixels into objects. Segments produced for a scene by seeded region growing are shown in Fig. 3. The parameters used for creating segments are scale, shape and compactness. By applying hit-and-trial method, parameter scale = 36, shape = 0.9 and compactness = 0.1 have given a better outcome though segmented objects were smaller as compared to the purposes of interest (eroded areas). All the three bands were given an equal weighting.

The classification of the image objects was executed by using membership functions, based on fuzzy logic theory combined with user-defined rules. Rule sets for classification are as follows: ExG has been used to extract eroded surface (possible landslides). For the eroded surface, objects have been trained such that all purposes which are having ExG value less than zero and the slope value higher than 25 are classified as the eroded surface. Some objects that belong to road class are misclassified as landslides due to the similarity in reflection with the eroded surface. That pixel can be removed by considering geometrical properties like length/width ratio.

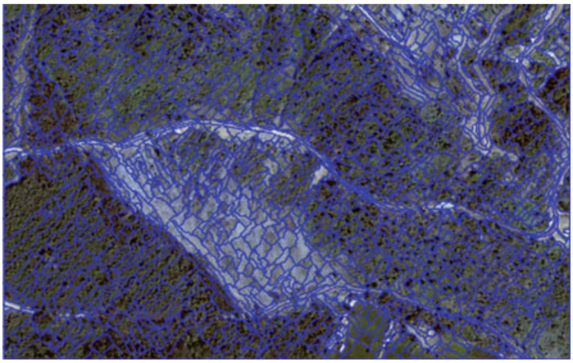

Fig. 3 Results of the segmentation

As the road is a linear feature, objects were trained such that all object which is having a length/width ratio higher than 3.5 should be classified as roads. To extract and discriminate both forest and sparse vegetation classes, GRVI indices are used. As forest will have high GRVI value (greater than 0.4) than sparse vegetation (0.1–0.2) and for rest, the average GRVI value was approximately 0.01–0.03. To detect freshly detached landslide, PAN is used as they tend to have a higher reflection, but they consist of positive ExG value due to low red band reflection. So all the objects which are having PAN value higher than 175 are classified as a freshly detached landslide, and they were later on merged with the landslide class. The detailed imagery is shown in Fig. 4b. As built-up is in a regular shape, so by using the geometrical properties of shape index, they are classified. A detached portion of land is represented as a yellow colour. A total of 13 landslides were observed from the imagery. While keeping the previous year imagery (Fig. 4a), there was a minimal trace of landslides. These figures help in understanding the magnitude of the disaster.

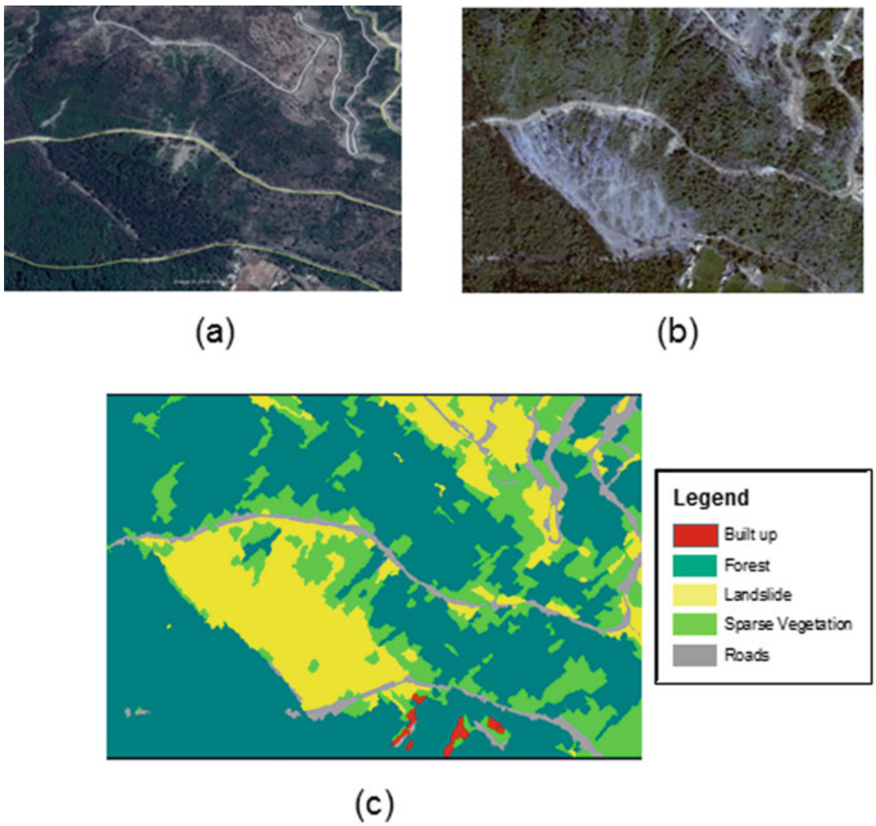

Fig. 4 **a** and **b** Sample image (May, 2016 and October, 2017) and **c** classified image

Fig. 5 Topography and drainage pattern of the study area

To gather more information regarding the occurrence of the landslide, few features have been obtained. By using the watershed delineation tool of ArcSWAT, drainage patterns are extracted, shown in Fig. 5. A drainage pattern is defined as topographical features from which a stream gets runoff, through flow, and groundwater flow which can be divided by topographic barriers called a watershed. By observing the drainage pattern keenly (Fig. 5), it has appeared that most of the reaches pass through the landslide area, which might indicate that more runoff passed through it during heavy rainfall of July 2017 which may further lead to detachment of surface. Also, slopes greater than 25° are more prone to a landslide as most of the detached area met this criterion.

One more observation is reflected from the imagery that landslide detachment occurs near to the road network. That confirms the frown upon that "anthropogenic activities are causing landslides". In the previous year image also, there were traces of landslides near the road network that is later on translated to greater disaster due to heavy rainfall, though there can be many other factors such as geological and hydrological behind this landslide other than above-discussed reasons.

4.2 Accuracy Assessment

Most of the classified scenes contain one central eroded area and sometimes a couple of small ones. To assess the consequences of the automated classification, they are compared to a manual classification of the nine scenes based on the same Google Earth scene. By observing Fig. 6, it can be seen that most of the landslides are mapped (location-wise) as compared to the reference, but the shape and size of the objects are slightly different. Overall accuracy is 96.99% if the conventional method of landslides assesses accuracy.

When comparing the total area of mapped landslides between the semi-automated object-based mapping and manual mapping, only minor differences are detected (Fig. 7). A slight trend towards overestimating the landslide area with OBIA compared to manual mapping can be recognised.

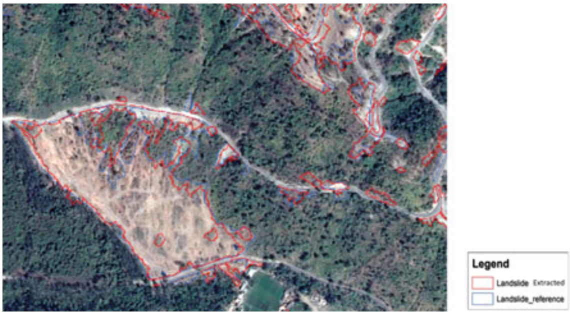

Fig. 6 Extracted and reference landslides

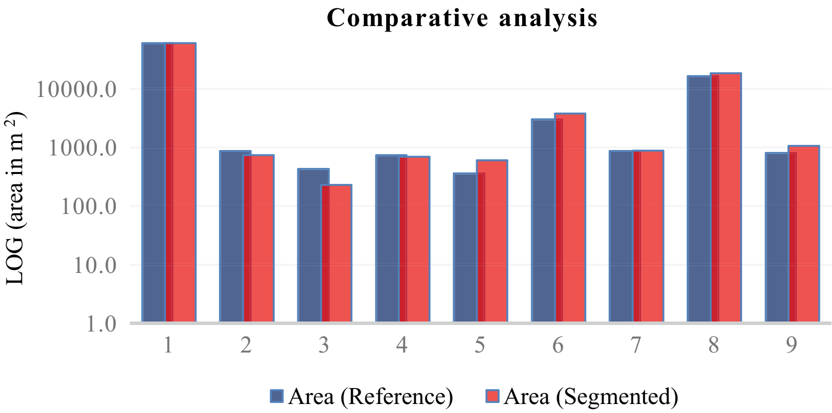

Fig. 7 Comparative analysis between the reference and extracted possible landslides

Accuracy assessment is performed on the area-based method included the various parameters into consideration such as (1) the relative area of an overlapped region to a reference object (RA_{or}), (2) the corresponding area of an overlapped region to a segmented object (RA_{os}), (3) the quality rate (qr) and (4) the SimSize. The outcomes reflect a different scenario. A total of nine samples are taken for the analysis. For parameters RA_{or} and $RA_{os,}$ extracted objects indicate a low accuracy of 79.77 and 75.44%, respectively.

The reason could be understood by observing Fig. 6 as extracted objects are very irregular in shape and continuity as compared to reference objects that lead to a smaller the overlay region which lowers the accuracy of these parameters. The qr parameter value lies between 0 and 1. The values close to zero indicate a perfect match, i.e. overlay and union areas are equal, while values close to one indicate an over- or under-segmentation, i.e. overlay region is tiny as compared to the union because object lies away from each other. The value obtained is 0.29, which indicates a functional similarity between overlay and union regions. The SimSize processes

Table 1 Accuracy assessment of Landslide area extraction

S. No	RA(or) %	RA (os) %	qr	SimSize
1.00	86	87	0.36	0.99
2.00	64	76	0.33	0.85
3.00	89	84	0.23	0.53
4.00	71	64	0.31	0.95
5.00	88	72	0.35	0.60
6.00	80	84	0.32	0.80
7.00	65	64	0.29	0.99
8.00	81	73	0.22	0.89
9.00	76	75	0.24	0.75
Overall	79.77	75.44	0.29	0.82

the similarity regarding the size of the *i*th segmented object and ranges between 0 and 1, with 1, being ideal parameters considering both geometric and spatial properties of the feature into consideration. SimSize value is 0.82, which indicates the geometrical similarities of objects are quite high.

The manual approach demonstrations gains for delineating single landslides or splitting up multiple landslides into smaller landslide regions. This is a challenge in OBIA since objects produced through segmentation rarely correspond to single landslides due to scale issues which correspond to over- or under-segmentation. Under-segmentation occurs when two or more segments may represent a single object, and over-segmentation occurs when a single segment may contain several objects, respectively (Clinton et al. 2008). Advanced split and merge algorithms could be used to refine the delineation of image objects, or manual editing can be done, but it is a tedious and time-consuming process. However, the creation of "meaningful" objects about a particular context or aim can be very complicated (Blaschke et al. 2014). Thus, instead of associating the absolute number of mapped landslides, the overlapping area was used for calculating the mapping accuracy in this study. Although results from manual mapping performed by local experts are often the only reference available, they cannot constitute an utterly accurate reference as their generation depends on various factors. Above-mentioned factors have to be well-thought-out when interpreting accuracy values (Table 1).

5 Uncertainty in Outcome

Remote sensing methods work on the basic principle of optics such as reflection, refraction and absorption of radiation. How any object will respond to a specific wavelength could be understood by its spectral reflectance curve. The reflected radiation is further converted to a brightness value and is a necessary input to automatic extraction of features. If the reflection curve of soil is seen, then few observation can be noted: (1) higher reflection for longer wavelength (Till 2.2 μm) and (2) absorption band (1.4, 1.9 and 2.2 μm) (Fabre et al. 2015). It implies that all the signification outcome lies in the longer wavelength. Now coming to the study, Google Earth imagery is used for feature extraction that comprises only visible bands, which indicates loss of valuable information as for soil reflection increases steadily towards longer wavelength in the visible region, but so does construction material such as concrete and asbestos. Due to this problem, a significant amount of misclassification can be observed between roads, built-up and possible landslides. It was the main reason behind the inclusion of barren land into a potential landslide. This caused uncertainty in the outcome.

As ancillary information, digital elevation model is used to map possible landslides. However, CartoDEM has a spatial resolution of 30 m which is larger than the spatial resolution of Google Earth 0.46 m. It dilutes the information for each pixel. The significant difference in spatial resolution of both layers makes the outcome from overlay operation unreliable. This error can be reduced to a great extent by using high-resolution stereo pair data such as IKONOS, Cartosat, but they carry a limitation of cost and availability within.

Object-based image analysis was used for the automatic extraction of various land uses/land covers; it does not promise to replicate the real scenario; it just helps in portraying a crude representation of reality. Main drawbacks of visual interpretation are the uncertainty of outputs, the subjectivity and the strict dependence on human expertise. The reference layer is prepared through manual mapping, which is generally accurate within the limits of image quality, is a very time-consuming process and also its level of accuracy depends on the efficacy of the user. This has to be considered when reading accuracy values. Reference layer (manually digitised) cannot be viewed as a real layer as landslide depends on the various geological, anthropogenic and hydrological factors which cannot be identified through visual interpretation. In this study, all of the elements which trigger the landslides are not extracted. So field survey is must to testify the outcomes.

6 Conclusion

The OBIA has been proven as a promising method for landslides identification and classification. An advantage of the OBIA approach, compared to a pixel-based classification, is that it copes with the salt–pepper noise of the high-resolution data, and also it considers spectral properties as well as shape and texture of the objects. In order to increase accuracy, more attention should be given to the classification rules and the type of data in the analysis. The lack of the DEM with a spatial resolution equivalent to the Google Earth and the lack of a more detailed lithological and geological map have brought many uncertainties in the classification process.

In accuracy assessment, the developed landslide detection algorithm achieved 79.77, 77.54, 29 and 82% for parameters RA_{or}, RA_{os}, qr and SimSize, respectively. Location-based accuracy parameter, also known as overall accuracy, reflects 96.7% accuracy. The massive difference between the outcomes is due to consideration of different factors in the analysis. Area-based accuracy methods give more reliable information as it captures both geometry and location into account, while the later focuses on the location only.

The study demonstrates that landslide mapping can be done by using open-source data with considerable accuracy.

References

Blaschke T, Hay GJ, Kelly M, Lang S, Hofmann P, Adding E (2014) Geographic object-based image analysis—towards a new paradigm. ISPRS J Photogram Remote Sens 87:180–191

Campbell JB, Wynne RH (2011) Introduction to remote sensing, 5th edn. The Guilford Press, New York, 667 pp

Casagli N, Cigna F, Bianchini S, Hölbling D, Füreder P, Righini G, Del Conte S, Friedl B, Schneiderbauer S, Iasio C, Vlckoh J, Greif V, Proske H, Granica K, Falco S, Lozzi S, Mora O, Arnaud A, Novali F, Bianchi M (2016) Landslide mapping and monitoring by using radar and optical remote sensing: examples from the EC-FP7 project SAFER. Remote Sens Appl Soc Environ 4:92–108

Clinton N, Holt A, Yan L, Gong P (2008) An accuracy assessment measure for object-based image segmentation. Int Arch Photogramm Remote Sens Spatial Inf Sci XXXVII(Part B4)

Cruden DM, Varnes DJ (1996) Landslide types and processes, Special Report, Transportation Research Board. Natl Acad Sci 247:36–75

De Blasio FV (2011) Introduction to the physics of landslides. Springer, Dordrecht, Heidelberg, London, New York

Dragut L, Blascke T (2006) Automated classification of landform elements using object-based image analysis. Geomorphology 81:330–344

Drăgut L, Eisank C (2010) ESP: a tool to estimate scale parameters for multi-resolution image segmentation of remotely sensed data. Int J Geogr Inf Sci 24(6):859–871

Fabre S, Briottet X, Lesaignoux A (2015) Estimation of soil moisture content from the spectral reflectance of bare soils in the 0.4–2.5 μm domain. Sensors 15:3262–3281

Fiorucci F, Cardinali M, Carlà R, Rossi M, Mondini AC, Santurri L, Ardizzone F, Guzzetti F (2011) Seasonal landslide mapping and estimation of landslide mobilization rates using aerial and satellite images. Geomorphology 129:59–70

Guo Z, Shao X, Xu Y, Miyazaki H, Ohira W, Shibasaki R (2016) Identification of village building via Google Earth images and supervised machine learning methods. Remote Sens 8:271

Guzzetti F, Mondini A, Mondini A, Cardinali M, Fiorucci F, Santangelo M, Chang K (2010) Landslide inventory maps: new tools for an old problem. Earth-Sci Rev 112:42–66

Hölbling D, Füreder P, Antolini F, Cigna F, Casagli N, Lang S (2012) A semi-automated object-based approach for landslide detection validated by persistent scatterer interferometry measures and landslide inventories. Remote Sens 4:1310–1336

Hölbling D, Friedl B, Eisank C (2015) An object-based approach for semi-automated landslide change detection and attribution of changes to landslide classes in northern Taiwan. Earth Sci Inf 8(2):327–335

Laliberte AS, Browning DM, Rango A (2012) A comparison of three feature selection methods for object-based classification of sub-decimeter resolution Ultracam-L imagery. Int J Appl Earth Obs 15:70–78

Malamud BD, Turcotte DL, Guzzetti F, Reichenbach P (2004) Landslide inventories and their statistical properties. Earth Surf Process Landforms 29:687–711

Mayr A, Rutzinger M, Bremer M, Geitner C (2016) Mapping eroded areas on mountain grassland with terrestrial photogrammetry and object-based image analysis. In: ISPRS annals of the photogrammetry, remote sensing and spatial information sciences, Volume III-5, XXIII ISPRS Congress, Prague, Czech Republic, vol 5, pp 137–144

Motohka T, Nasahara KN, Oguma H, Tsuchida S (2010) Applicability of green-red vegetation index for remote sensing of vegetation phenology. Remote Sens 2:2369–2387

Mulders MA (1987) Remote sensing in soil sciences. Elsevier Science Publishers B.V, The Netherlands

Platt RV, Rapoza L (2008) An evaluation of an the object-oriented paradigm for land use/land cover classification. Prof Geogr 60:87–100

Rau JY, Jhan JP, Lob CF, Linb YS (2011) Landslide mapping using imagery acquired by a fixed-wing UAV. In: International archives of the photogrammetry, remote sensing and spatial information sciences, Volume XXXVIII-1/C22, ISPRS Zurich Workshop, Zurich, Switzerland, pp 195–200

Santurri L, Carlà R, Fiorucci F, Aiazzi B, Baronti S, Cardinali M, Mondini A (2010) Assessment of very high-resolution satellite data fusion techniques for landslide recognition. Int Arch Photogramm Remote Sens Spat Inf Sci 38(B7):492–496

Scaioni M, Longoni L, Valentina Melillo V, Monica Papini M (2014) Remote sensing for landslide investigations: an overview of recent achievements and perspectives. Remote Sens, 6, 1-x manuscripts. https://doi.org/10.3390/rs60x000x

Selby MJ (1993) Hillslope materials and processes. Oxford University Press, Oxford

Sharma N (2017) Frequent landslides in Uttarakhand worries scientists. Hindustan Times, July 17

Taylor P, Montaghi A, Larsen R, Greve MH (2015) Accuracy assessment measures for image segmentation goodness of the Land Parcel Identification System (LPIS) in Denmark. Remote Sens Lett 4(10):946–955

Tsai F, Hwang JH, Chen LC, Lin TH (2010) Post-disaster assessment of landslides in southern Taiwan after 2009 Typhoon Morakot using remote sensing and spatial analysis. Nat Hazard Earth Syst 10:2179–2190

Weidner U (2008) Contribution to the assessment of segmentation quality for remote sensing applications. In: Proceedings of the 21st congress for the International Society for Photogrammetry and Remote Sensing, 3–11 July, Beijing, China

Woebbecke DM, Meyer GE, Von Bargen K, Mortensen DA (1995) Colour indices for weed identification under various soil, residue, and lighting conditions. Trans ASAE 38(1):259–269

Yu L, Gong P (2011) Google Earth as a virtual globe tool for earth science applications at the global scale: progress and perspectives. Int J Remote Sens 33:366–3986

Zhan Q, Molenaar M, Tempfli K, Shi W (2005) Quality assessment for geospatial objects derived from remotely sensed data. Int J Remote Sens 26(14):2953–2974